Scandinavian Journal of Forest Research

ISSN: 0282-7581 (Print) 1651-1891 (Online) Journal homepage: https://www.tandfonline.com/loi/sfor20

Photogrammetric measurement of tree stems from vertical fisheye images

Adilson Berveglieri, Antonio Tommaselli, Xinlian Liang & Eija Honkavaara

To cite this article: Adilson Berveglieri, Antonio Tommaselli, Xinlian Liang & Eija Honkavaara (2017) Photogrammetric measurement of tree stems from vertical fisheye images, Scandinavian Journal of Forest Research, 32:8, 737-747, DOI: 10.1080/02827581.2016.1273381

To link to this article: https://doi.org/10.1080/02827581.2016.1273381

Accepted author version posted online: 15 Dec 2016.
Published online: 30 Dec 2016.

SCANDINAVIAN JOURNAL OF FOREST RESEARCH, 2017
VOL. 32, NO. 8, 737–747
https://doi.org/10.1080/02827581.2016.1273381

Taylor & Francis
Taylor & Francis Group

Photogrammetric measurement of tree stems from vertical fisheye images

Adilson Berveglieri[a], Antonio Tommaselli[a], Xinlian Liang[b,c] and Eija Honkavaara[b]

[a]Department of Cartography, Universidade Estadual Paulista – UNESP, Presidente Prudente, Brazil; [b]Finnish Geospatial Research Institute FGI, National Land Survey of Finland, Helsinki, Finland; [c]Centre of Excellence in Laser Scanning Research, Academy of Finland, Helsinki, Finland

ABSTRACT

Forest variables are typically surveyed using sample plots, from which parameters for large areas are estimated. The diameter at breast height (DBH) is one of the main variables collected in the field and can be used with other forest measures. This study presents an automatic technique for the mapping and measurement of individual tree stems using vertical terrestrial images collected with a fisheye camera. Distinguishable points from the stem surface are automatically extracted in the images, and their 3D ground coordinates are determined by bundle adjustment. The XY coordinates of each stem define an arc shape, and these points are used as observations in a circle fitting by least squares. The circle centre determines the tree position in a local reference system, and the estimated radius is used to calculate the DBH. Experiments were performed in a sample plot to assess the approach and compare it with a technique based on terrestrial laser scanning. In the validation with measurements collected on the stems using a measuring tape, the discrepancies had an average error of 1.46 cm with a standard deviation of 1.09 cm. These results were comparable with the manual measurements and with the values generated from laser point clouds.

ARTICLE HISTORY
Received 7 March 2016
Accepted 10 December 2016

KEYWORDS
DBH; bundle adjustment; circle fitting; vertical images; photogrammetry

Introduction

Field data surveyed in forest sample plots are fundamental to achieving several purposes, for example, monitoring of tree growth, biomass estimation, timber volume estimation, and forest inventory. When trees are individually located and measured, more reliable information can be obtained to describe the sample plot. Moreover, tree positions from the field can also be located in high-resolution aerial images, and individual tree identification contributes to remote sensing-based studies.

An on-site ground survey in sampling plots typically records species and stem diameters at a 1.30 m height, also known as the diameter at breast height (DBH). The DBH is an essential variable because it correlates with many other quantities that are more difficult to measure, such as the tree height, wood volume, and biomass. Manual measurement techniques are usual; however, they are time-consuming and only produce partial knowledge of the forest structure. Liang et al. (2014) commented about the lack of an efficient solution for measuring individual trees. Typically, a rangefinder and a bearing compass are used as measuring devices. In addition to these, other devices, such as a relascope laser and calliper systems, have been developed; however, they still depend on manual measurements and are labour intensive.

Terrestrial laser scanning (TLS) has been used for forestry applications to provide point clouds that describe 3D structures. Several approaches have used TLS for stem diameter estimation (Watt & Donoghue 2005; Vastaranta et al. 2009; Lovell et al. 2011; Lindberg et al. 2012; Liang & Hyyppä 2013; Ringdahl et al. 2013) and characterized other variables such as tree density, canopy cover, and heights (Henning & Radtke 2006; Dassot et al. 2011). The detection of stems in point clouds aims at locating the spatial position for individual modelling and for extracting dendrometric variables. However, the cost of TLS hardware is considerable, and the use of TLS requires expert knowledge, which limits the use of TLS in daily practice.

Recent advances in digital imaging sensors and photogrammetric processing technologies have greatly improved remote sensing techniques based on optical images, which enables measurement of 3D coordinates and point clouds in forest environments with an accuracy comparable to TLS (Liang et al. 2014). Direct and indirect methods are the two main approaches for estimating forest parameters. Indirect methods based on remote sensing using light-weight equipment are generally more cost efficient and easier to operate than the direct methods based on manual measurements. Indirect measurements based on images enable estimates of tree attributes such as height (Korpela et al. 2007), diameter (Clark et al. 2000; Forsman et al. 2012; Liang et al. 2014) and volume (Hapca et al. 2007), as well as stem mapping (Dick et al. 2010; Rodríguez-García et al. 2014; Liang et al. 2015). These parameters are typically used to understand how forests grow and develop.

The work by Hapca et al. (2007) used two digital images taken from two stations with convergence, defining an intersection angle of 90° to reconstruct the 3D shape of standing trees. Forsman et al. (2012) proposed a methodology to estimate DBH with a system composed of five digital cameras

CONTACT Adilson Berveglieri adilsonberveg@gmail.com Department of Cartography, Univ Estadual Paulista – UNESP, Rua Roberto Simonsen, 305, 19060-900, Presidente Prudente, Brazil

attached to a calibrated rig. The developed method generated point clouds using the scale invariant feature transform (SIFT) technique in multiple images in combination with epipolar line geometry. A projection of the point cloud to a simulated ground plane was followed by circle fitting to the remaining points. Forsman et al. (2016) obtained a root mean square error (RMSE) of 2.8–9.5 cm for trees located up to a distance of 7 m. In mapping forest sample plots, Liang et al. (2014) presented an approach to generate terrestrial point clouds using an uncalibrated hand-held camera. The technique achieved an RMSE of 2.39 cm in DBH estimates of individual trees, results which are acceptable for forest applications and close to results obtained with TLS. In Liang et al. (2015), a sample plot was mapped and different landscape/portrait image configurations were used. Five image point clouds from two mapping paths located inside and outside of the plot were compared. The overall detection accuracies of the image-based point clouds were 60–84%. The bias% and RMSE% of the DBH estimation were 3.6–8.5% and 8.0–18.9%, respectively.

The feasibility of using fisheye cameras in collecting forest data has been investigated in previous studies. Fisheye lenses increase the possibility of obtaining images in places of difficult access and allow a large ground coverage area. Hemispherical images of forest canopy have been widely used since Evans and Coombe (1959) showed that fisheye images could be used to study sunlight penetration through forest environments by superimposing the track of the sun on the images. This type of hemispherical system is more compact and simpler than a system with multiple cameras, reducing the time demanded to calibrate equipment and possible errors propagated in the process. Fisheye optics systems provide images with a large field of view around the camera using only one image; however, the images have large scale variations caused by the imaging geometry and a consequent loss of resolution. Thus, the camera must be accurately calibrated using a specific model for the fisheye lens (Schneider et al. 2009; Marcato Junior et al. 2015).

There are few studies of using multiple fisheye images to measure forest structure. Rodríguez-García et al. (2014) performed a study based on stereoscopic hemispherical images using the device MU2005-01738. Tree positions were determined with an RMSE of 23 cm, and DBHs were measured with an RMSE of 1.51 cm. However, several camera positions were needed to generate the horizontal fisheye stereo models using this technique. Herrera et al. (2011) proposed a fisheye stereovision method for forest environments combining a step for image segmentation (to separate textures of interest) with the matching process. The final decision about the correct match was made based on a weighted fuzzy similarity approach; the objective of the methodology was to compute disparity maps of the tree stems.

The main objective of this investigation is to present a study for the automation of a data acquisition process using panoramic optical images. A technique based on the fisheye lens is used to collect multi-scale images in a forest plot. Only a minimum of three images displaced vertically but captured from the same planimetric camera station are required to apply the approach, which do not need walking inside or outside of the sample plot and therefore improve the fieldwork efficiency. Several variables can be obtained from the scenes, including samples of diameters along the stems, ground texture, and shadows as well as the position and spatial distribution of the trees. Furthermore, the acquired images are a permanent record of a forest sampled plot and allow subsequent data analysis over time. The feasibility of this technique was previously assessed using manual techniques to locate and measure image points on stems (Bergveglieri et al. 2014).The encouraging results motivated us to automate the approach. In this paper, all image points and stems were extracted by automatic techniques. Furthermore, the results of the proposed technique were evaluated using field measurement and compared with an approach based on TLS.

Materials and methods

In general, tree stems present cylindrical or conical shapes whose vertical development depends on the environmental conditions. Within a small section of stem, the difference between cylindrical or conical shapes is insignificant except for at the tree base and top. Therefore, a regular cylinder can be adopted as a geometric model.

Based on this assumption, distinguishable points of the stem surface within a range can be extracted and used to determine a circle approximately 1.3 m in height. The concept is that the XY planimetric coordinates of these points in the object space describe an arc shape when projected onto a horizontal reference plane, as depicted in Figure 1. Then, a circle can be fitted with the planimetric coordinates to determine the centre C and its radius r (or diameter = $2r$).

To use this concept, an automatic approach was developed to identify tree stems using optical images, extract points on stems, determine their 3D coordinates, and estimate the DBH along with circle fitting. The entire procedure consists of the following main steps: camera calibration, image acquisition, image processing, bundle adjustment (BA), and circle fitting.

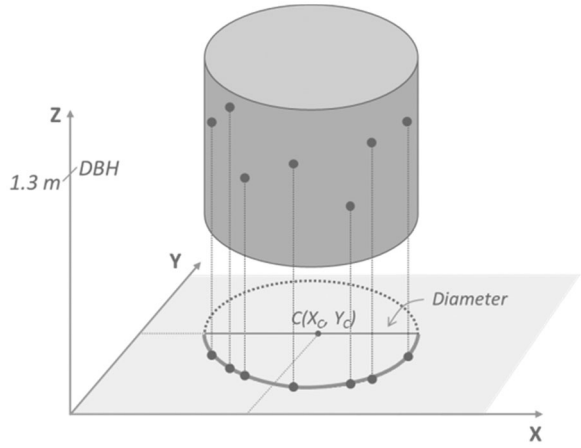

Figure 1. The planimetric coordinates of the points around $Z = 1.3$ m describe an arc in the reference plane and can be used to fit a circle and determine its diameter.

Camera calibration

Camera calibration is performed to determine the interior orientation parameters (IOPs), which must be accurate and stable. In the proposed technique, a fisheye or wide-angle lens is used to collect panoramic images. Because a fisheye lens does not follow the collinearity equations due to its internal geometry, a suitable model should be used, for example, an equidistant, equisolid-angle or orthographic model (Schneider et al. 2009), in which the Conrady-Brown model lens distortion parameters (Brown 1971) should be included. The system of linearized equations can be solved using the least squares method considering constraints imposed on the ground coordinates, object distances or exterior orientation parameter (EOP) observations. More details will be given in section "Results".

Image acquisition

The technique to collect images and generate multi-scale models was originally designed by Tommaselli and Berveglieri (2014) and adapted for forest applications. The imaging system is composed of a fisheye camera attached to a telescopic pole, which is positioned among trees to acquire vertical images. In down nadir viewing, these images are acquired at suitable positions (X, Y) at different heights, varying only Z above the ground, as depicted in Figure 2. Planimetric camera positions remain unchanged except for small displacements caused by pole movements. Previous experiments performed by Tommaselli and Berveglieri (2014) demonstrated that three images can provide geometric quality sufficient for an accurate BA.

The vertical camera displacement ensures that the same trees are visible in all images without significant changes in stem aspect, which facilitates automatic tree detection and image matching. This is not guaranteed when taking pictures using a horizontal camera displacement, when many occlusions are likely to occur due to viewpoint changes. Thus, many images are needed to generate suitable overlaps and coverage. With the proposed technique, the parallaxes caused by changing the viewpoint occurs in the vertical direction and the upward vertical movement increases the field of view, ensuring the image overlap and viewpoint changes necessary to perform forward intersection. Consequently, fewer images are needed. Moreover, maintaining the same planimetric position makes the measurement using this technique faster because there is no need to change the measurement position for each new image acquisition.

Image processing

The next step is to automatically extract distinguishable points from the stems and match them in all images. Figure 3 shows the stem aspect in a vertical image considering the scheme in Figure 2. Radial lines converging to the image centre can be observed.

For stem segmentation, a smoothing step with a median filter (e.g. large window 35×35 pixel) to eliminate small details is performed, followed by and automatic grey level segmentation. Having illumination differences in the images, two thresholds must be used separately: one to segment dark stems (shadowed) and another to segment light stems. In the current implementation, the Yen's method (Yen et al. 1995) and minimum error thresholding (Kittler & Illingworth 1986) are being used. Automatic thresholds are typically based on image histogram analysis and they can be used as a first segmentation step. Thus, an initial segmentation is made by combining the results from both thresholds in a single image, which is a binary image with one (1) representing areas that are likely to have stems and zero (0) for background area. This step is not sufficient to segment stems because unwanted elements may still appear. Then, a radial search for stems is performed. This search uses a radial pixel chain with origin in the image centre and rotating in clockwise direction. A radial segment is maintained if it has more connected pixels than a predefined number. This Boolean operation maintains all significant radial structures and eliminates small segments.

This makes feasible to extract the main radial structure of each stem. At least one linear structure is required but several can be located. Next, windows are opened around these radial structures, limiting the space for point extraction over the stems. The window size must be large enough to cover the stem width, which is defined in pre-processing step. It is important to note that such windows do not need to be limited to the stem contour and may exceed their edges. Local windows are only used to ensure that

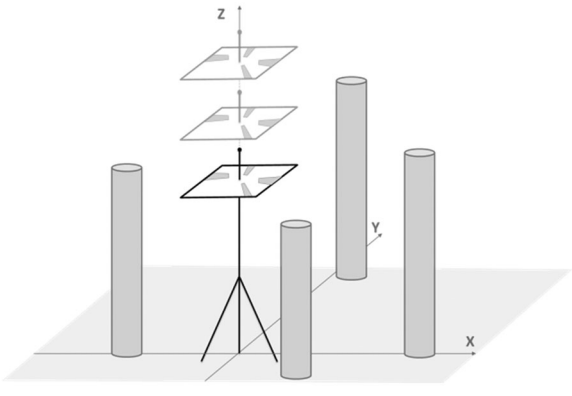

Figure 2. Acquisition of vertical images at different heights.

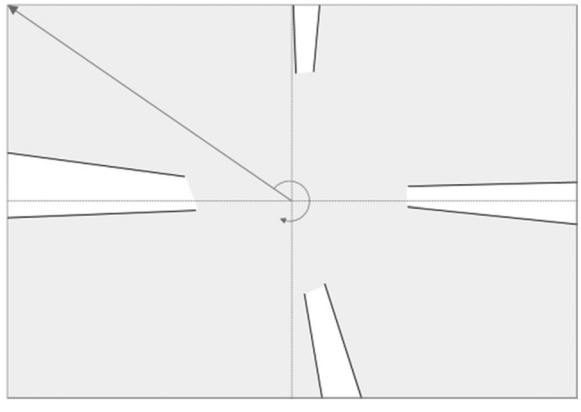

Figure 3. Nadir view that enables a radial search for vertical stems.

photogrammetric points will be extracted over the stems. This step makes feasible the application of local image enhancement and keypoint extraction only over regions of interest.

As the set of images contains different scales and can present rotation variation, the SIFT technique (Lowe 2004) can be used to extract conjugate points in the images. The SIFT correspondence is established using feature-based matching (FBM) of keypoints. Many correct matches are ensured due to the application of FBM with SIFT (restricted to image patches containing stems) along with the establishment of correspondence for three images (each point having three intersection of rays). The angle of the keypoint in relation to the image centre is used as an attribute for stem identification for later segmentation of the 3D points belonging to each stem.

Bundle adjustment

The points extracted from the images are used to estimate their 3D coordinates via BA. The extracted points are considered as tie points in the BA, which is performed in an arbitrary system (first image as reference) without ground control points. To achieve this, the EOPs must be estimated with accurate values, and the image matching must be accurately established with reliable matches. The heights of the camera stations are accurately measured during image acquisition for use as constraints in the image orientation procedure. The attitude parameters (ω, φ, κ) are considered unknowns.

The images have approximately the same planimetric position and attitude but different heights, which results in image scale changes. The EOPs of the lowest image are set with six absolute constraints to the camera position ($X_0 = 0$, $Y_0 = 0$, $Z_0 =$ camera height) and the camera attitude angles ($\omega = 0$, $\varphi = 0$, $\kappa = 0$). For the EOPs of the second and third images, weighted constraints are imposed with respect to height and small variations due to vertical displacements of the pole when it is raised (more details in section "Data processing"). The set of images can then be oriented by BA using an arbitrary local reference system. A local reference system is usually adopted for surveying of individual trees because of the difficulties for accurate GPS surveying inside dense forests. When a georeferenced tree position map is required, the local reference system can be transformed to a global system using two control points appearing in the images or the geographic coordinates of the acquisition station and the azimuth of the camera axis.

BA uses the least squares method to solve a system of non-linear equations in which the image coordinates of the tie points are the observations and the EOPs and ground coordinates of the tie points are the unknowns. In this technique, the combined adjustment method for BA is used with the equidistant model for fisheye lenses, as implemented by Marcato Junior et al. (2015).

Circle fitting

The BA with stem points as tie points yields a set of 3D object coordinates. Their planimetric coordinates describe a curve that can be fitted with a circle by least squares adjustment. Formally, a circle can be defined by its centre $C(X_C, Y_C)$ and radius r in a non-linear mathematical model (1). If the model is linearized, the least squares method can be used to estimate the parameters from redundant observations. Thus, the XY object coordinates (around DBH) are used as observations, and X_C, Y_C, and r are the parameters to be estimated. A minimum of three non-vertically aligned points (or observations), as well as initial values, must be provided for the three parameters. Weighting of observations is not necessary because the object points have approximately the same accuracy because all tie points are generated by photogrammetric intersection using three rays. The solution is achieved by least squares adjustment (Mikhail et al. 2001, p. 396). After the iterative algorithm converges, the circle parameters are determined. Then, the stem diameter can be calculated from the estimated radius r by

$$(X_i - X_C)^2 + (Y_i - Y_C)^2 = r^2, \quad (1)$$

where (X_i, Y_i) are $n \geq 3$ points to be fitted in relation to the central point $C(X_C, Y_C)$.

There exist other methods for circle fitting which do not require initial values, for example, linear models by parameter grouping (Coope 1993). In this approach, an iterative method was adopted to rigorously adjust observed data and parameters (Mikhail et al. 2001, p. 396) using the circle equation. Since 3D stem points are available, their coordinates are used to calculate initial values for the unknowns.

Results

The experiments were conducted in a mature forest plot in Masala (60.15°N, 24.53°E), southern Finland. The test area has a tree density of 278 stems/ha (DBH > 10 cm). Sapling and shrubs also grow on the plot. The tree species in the test area are Scots pine (*Pinus sylvestris L.*) and birches (*Betula sp. L.*) (Figure 4).

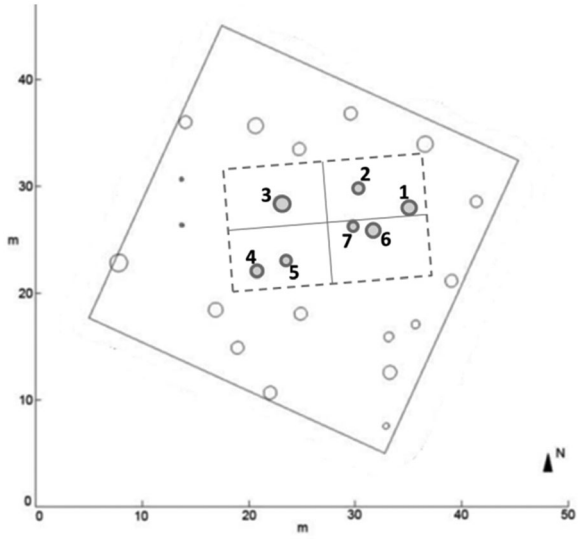

Figure 4. Forest plot used in the experiments. The numbered circles inside the dashed rectangle represent the assessed stems.

The forest was measured with the fisheye cameras and TLS at approximately the same location. Results from two data sets were compared to evaluate the performance of the tree measurement using the fisheye camera.

TLS data acquisition

The TLS point cloud was collected as a reference for the evaluation of the image-based point cloud. The study area was scanned using a Leica HDS6100 TLS® (Leica Geosystems AG). The distance measurement accuracy of the scanner is ±2 mm at 25 m distance, and the maximum measurement range is 79 m. The study area was scanned using the single-scan approach. A full field-of-view (360° by 310°) scan was performed. The forest area was scanned without pre-scan preparations such as the removal of lower tree branches or the clearance of undergrowth (Liang et al. 2014).

The TLS data set was processed using the robust modelling method (Liang et al. 2012) to estimate tree attributes. A local coordinate system was established for each laser point in its *kNN* neighbouring space, *k* being 100 in this test. A stem surface is typically vertical and has a planar shape. Points on such a surface were selected as potential stem points, and tree stem models were built from these possible stem points. A series of 3D cylinders were used to represent changing stem shapes. To eliminate influences of noise, for example, branch points, each point was weighted in the modelling process. The weight was calculated from the Tukey estimator. The larger the residual, the smaller is the weight. The DBH and location of the stem were estimated from the cylinder element at the breast height, and the tree map was constructed based on these stem locations and DBH estimates.

Table 1. Technical details of the fisheye camera.

Elements	Specification
Camera model	Nikon D3100
Nominal focal length	8 mm (Bower SLY 358N fisheye)
Pixel size	5.0 µm
Sensor dimensions	CMOS APS-C (23.1 × 15.4 mm)
Image dimensions	4608 × 3072 pixels

Fisheye camera calibration and image acquisition

A Nikon D3100 digital camera with a fisheye lens (specifications in Table 1) was used to collect the images in the forest plot. The camera had been previously calibrated in a terrestrial calibration field composed of coded targets of ArUco form, proposed by Garrido-Jurado et al. (2014) and adapted for camera calibration by Silva et al. (2014), as shown in Figure 5.

Twelve images were acquired from three camera stations using different positions and rotations to reduce correlation in the estimation process by self-calibrating BA. The target corners were automatically extracted for use as observations in a BA, along with their ground coordinates. The camera calibration project was configured in the calibration multi-camera (CMC) software (developed in-house by Ruy et al. (2009) using the equidistant model (2) adapted by Marcato Junior et al. (2015)).

$$x' = x_0 + \Delta x - f.\frac{X_0}{\sqrt{X_0^2+Y_0^2}}.\arctan\left(\frac{\sqrt{X_0^2+Y_0^2}}{Z_0}\right),$$
$$y' = y_0 + \Delta y - f.\frac{Y_0}{\sqrt{X_0^2+Y_0^2}}.\arctan\left(\frac{\sqrt{X_0^2+Y_0^2}}{Z_0}\right), \quad (2)$$

where (x', y') are the image point coordinates, (x_0, y_0) are the principal point coordinates, Δx and Δy are the effects of lens distortion (radial and decentring distortion), f is the focal length, and (X_0, Y_0, Z_0) are the camera perspective centre coordinates in the local reference system. Table 2 presents the estimated IOPs.

Vertical fisheye images were collected as described in Section "Image acquisition". Figure 6(a) shows the imaging system positioned in the plot, and Figure 6(b) provides an example of a fisheye image acquired in nadir view. Three

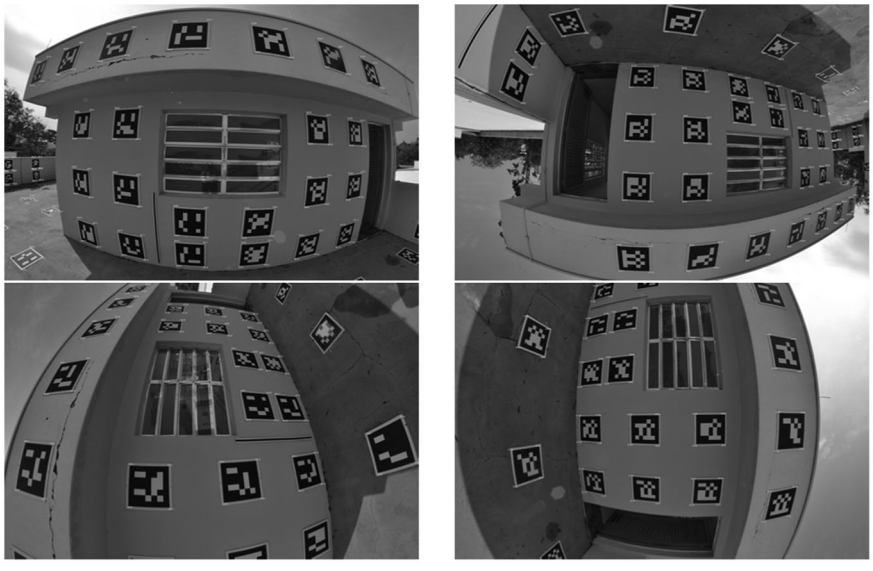

Figure 5. Example of fisheye images taken in the camera calibration field composed of ArUco coded targets.

Table 2. IOPs estimated by the BA with the equidistant model.

Parameter	Value	Standard deviation
f (mm)	8.3526	0.00306794 (±0.61 pixels)
x_0 (mm)	0.0701	0.00119047 (±0.24 pixels)
y_0 (mm)	−0.1308	0.00110620 (±0.22 pixels)
K_1 (mm^{-2})	4.50×10^{-4}	6.69×10^{-6}
K_2 (mm^{-4})	3.99×10^{-7}	8.50×10^{-8}
K_3 (mm^{-6})	1.09×10^{-10}	3.54×10^{-10}
P_1 (mm^{-1})	9.27×10^{-6}	1.99×10^{-6}
P_2 (mm^{-1})	-9.69×10^{-6}	2.22×10^{-6}
a posteriori *sigma*	0.98	(a priori *sigma* = 1)

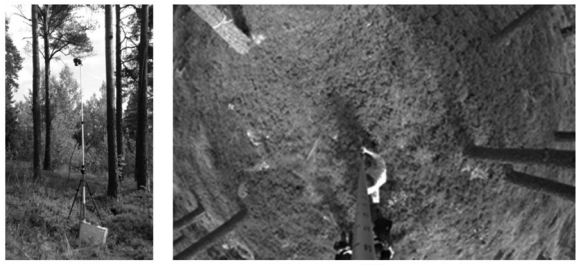

Figure 6. Imaging system positioned within the site. Example of a fisheye image in nadir view.

images were taken at three different heights above the ground: 3.95, 4.30, and 4.55 m. These heights were recorded for use in the BA as constraints. Only one tripod station with three images was used for the experiments because similar results were achieved when the technique was applied in other areas. Therefore, the objective of this study was to describe the methodology of acquisition and photogrammetric data processing using a practical application, to perform an accuracy assessment with the set of images and to compare with existing laser scanning results.

Data processing

The procedure described in Section "Image processing" was applied to automatically extract stem points. Figure 7 shows a sequence of partial results obtained during this procedure. An image converted to grey levels is shown in Figure 7(a).

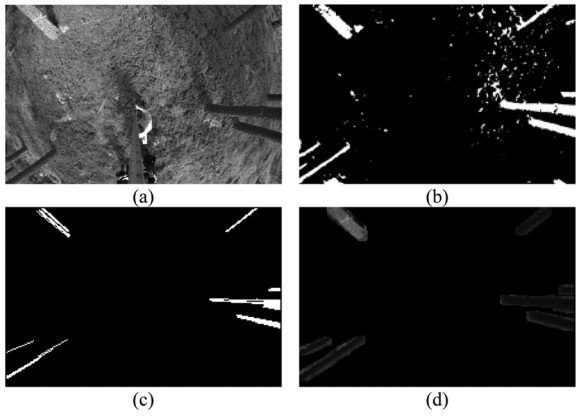

Figure 7. (a) Fisheye image in grey levels. (b) Thresholding and binarization. (c) Search for radial structures. (d) Windows approaching the stems.

This image was smoothed with median filter (with a 35×35 moving window). Next, two automatic local thresholds were applied using both the Yen (Yen et al. 1995) and minimum error (Kittler & Illingworth 1986) methods with radius = 15 pixels (default) to locate the stems and generate a binary image. Figure 7(b) displays the resulting image with the stem detection. However, other undesirable features may also appear, as can be observed in Figure 7(b). Thus, the search for radial alignments (or straight lines) in the scene allows a segmentation refinement to separate the stems only, as seen in Figure 7(c). This step was performed using the search for continuous segments (or sequence of pixels). Then, windows can be opened around the alignments, which greatly reduces the image patch needed to extract points from stems, as presented in Figure 7(d). It is important to observe that the region of the image where the telescopic pole appears is the same in all images; therefore, this region can be automatically labelled and excluded from the segmentation procedure.

In the next step, the SIFT technique was applied locally. If necessary, local enhancement can also be performed to improve the image contrast. The SIFT keypoint detector software, available from Lowe (2005), was applied to triplets of image patches selected in the previous steps. Figure 8(a) shows SIFT matches for the parts of two images within the matching windows that limit the search space around the stems.

The image coordinates of all detected points and their conjugates were inserted into a photogrammetric project for use as tie points (observations) in a BA. Calibrated IOPs and initial EOPs were also used in the BA. The initial values of the EOPs were based on measurements obtained during image acquisition and inserted as weighted constraints. These weights considered movements of the camera station and the relative accuracy of the measurements as follows:

- Six absolute constraints were imposed on the EOPs of the first image (the lowest image defined the origin and orientation in a local reference system).
- The heights (Z) of the second and third images were constrained with a standard deviation of $\sigma = 1$ mm and the XY coordinates of the perspective centre were constrained with a standard deviation of $\sigma = 5$ cm because small variations are expected due to the vertical displacement of the pole. The attitude parameters were configured as unknowns, which does not affect the results.

A standard deviation of $\sigma = 0.5$ pixels was defined for the image measurements. Then, the BA was computed with the CMC software using the equidistant model for fisheye lenses. The EOPs of the three images and the 3D coordinates of the tie points (with three ray intersection) were simultaneously estimated. An arbitrary reference system was defined considering the planimetric position of the telescopic pole as the origin, and the ground coordinates of the tie points were thus determined in this local reference system. As a result, an a posteriori *sigma* of 1.54 was achieved in the BA (with a priori *sigma* = 1). Figure 8(b) displays a 3D point cloud generated with tie points in the BA for the stem from

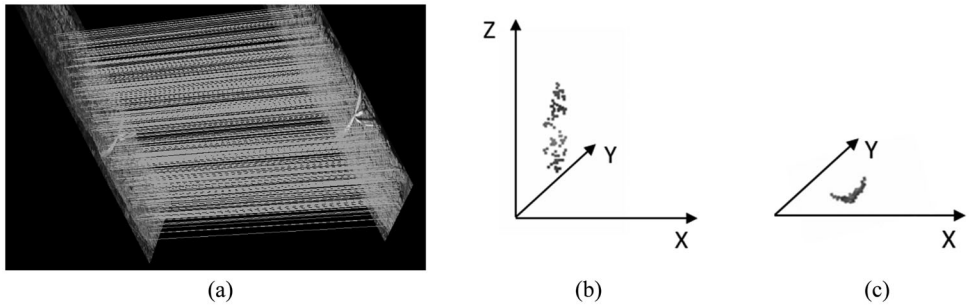

Figure 8. (a) Matched pairs of keypoints extracted with SIFT at two corresponding windows. (b) 3D point cloud estimated by the BA. (c) Arc shape generated with the *XY* coordinates in the object space.

Figure 8(a). An arc shape can be observed in Figure 8(c) for the XY coordinates that determine the stem curve. Next, a set of object points (tie points in a neighbourhood of the DBH, 1.3 m ± 0.2 m height) on each stem was used to adjust a circle by the least squares method, from which each stem centre and radius were determined using the XY object coordinates. A Matlab script was implemented to perform the circle fitting.

The mathematical model of a circle is a non-linear equation that requires initial values to estimate the parameters of the stem centre (*Xc*, *Yc*) and radius *r* by the least squares method. The initial value of the radius can be estimated as half of the largest length among the stem points. The stem centre position (*Xc*, *Yc*) can be estimated based on the point nearest to the origin of the reference system (0, 0) plus the radius. Using the planimetric coordinates as observations in the system of equations, the adjustment procedure is iteratively performed to achieve the solution. All planimetric coordinates are considered to have the same weight in this adjustment. After convergence, the radius is used to determine the DBH. Figure 9 shows three examples of circles estimated around the DBH by the fisheye technique. Both fitted circles and planimetric coordinates can be observed in a local reference system, as plotted in Figure 10.

As seen in Figure 9(a–c), circles can be estimated with different numbers of points. Figure 9(a) shows several points covering the width of the stem visible in the image, Figure 9(b) exemplifies a situation with points concentrated in a cluster with a few distant points, and Figure 9(c) displays a few points forming an arc shape sufficient to determine a circle. These examples show the results of the automatic point extraction, which depends on the stem surface features. Thus, the lighter part of a stem can generate more points than the dark part, as shown in Figure 9(b). However, the horizontal distribution around the DBH is more important to capture the stem curvature for circle fitting than the number of points. The initial approximate values for the central position ensure convergence and good geometric quality for a correct circle determination.

Figure 10 shows all the stems (circles in scale) covered by the camera footprint that were used to estimate their DBHs and their positions in a local reference system. The estimated centre of each stem defines the spatial location within the plot.

Discussion

An assessment on the accuracy of the estimated tree position can also be done based on the theoretical precision of the photogrammetric tie points coordinates computed with BA. Besides the orientation of each image, this procedure determines the 3D point coordinates and their precision. The analysis of the standard deviations can provide estimates for the positional errors when mapping trees, since the tree position will be defined by the circle centre, estimated from 3D photogrammetric points. Figure 11 shows a graphical representation of the standard deviations against the distance from the camera station to the trees. The graph depicts the planimetric and altimetric errors considering only the sets of 3D points over the seven stems analysed in this paper.

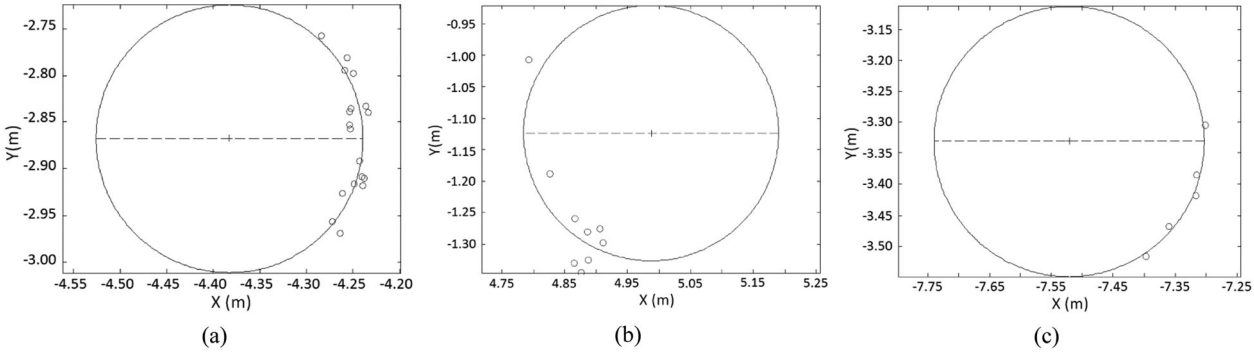

Figure 9. Examples of circles fitted around the DBH using the *XY* ground coordinates of points extracted from stem surfaces.

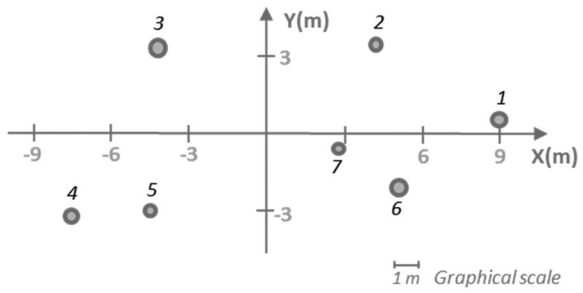

Figure 10. DBHs and stem position estimated in a local reference system.

The errors in planimetric positions ranged from 3.5 to 7.5 cm, depending on the distance between camera and each tree, while the errors in altimetry indicated smaller standard deviations varying between 3.0 and 5.2 cm. Planimetric errors in this procedure are a function of the distances from the camera to the object and can be compared to depth errors in conventional photogrammetry. Thus, this error will increase with the distance because the angles of the intersecting rays are reduced according to the base/depth ratio (see Krauss 1993, p. 27). Altimetric errors are smaller because they depend mainly on the image measurement error and on the image scale at that point. These errors do not significantly affect the tree position, and therefore, the mapping can be produced with an error less than 7.5 cm for a distance of approximately 10 m, which is acceptable for large scale mapping.

Table 3 presents the number of points used to estimate each DBH as well as the a posteriori *sigma* and the standard deviations (σ) of the three parameters (X_C, Y_C, r) obtained from the circle fitting by least squares.

The number of points depends on the characteristics of each stem. The results demonstrate that a precise adjustment can be achieved in the parameter estimation even using only a few points. The a posteriori *sigma* values (Mikhail et al. 2001, p. 414; Wolf et al. 2014, p. 513) of the seven stems indicate an overall precision of approximately 0.002 m in the best circle fitting and 0.015 m in the worst fitting, which represents a dispersion of less than 2 cm in the adjustment. The stem centres were estimated with standard deviations from 0.8 to 3.1 cm in X and from 0.1 to 4.7 cm in Y, which represent the precision in the determination of the stem positions. For the radius estimation, the standard deviations varied from 0.4 to 2.4 cm, generating an average value of 1.24 cm.

To validate the results, each stem perimeter was manually measured with a measuring tape at the height of 1.30 m, from which the diameter was calculated. In Table 4, the second column presents the differences between the stem diameters estimated by the photogrammetric technique and the directly measured stem diameters. The third column in Table 3 shows the distance from the camera station to the stem, which ranged from 2.60 to 9.01 m

A comparison of results was performed to assess the discrepancies when using the proposed technique. The largest discrepancies were obtained for stems 1 and 4, which were the most distant (>7.70 m) from the camera station and also had fewer extracted points. In contrast, stem 1 resulted in the smallest difference (~0.5 cm), although it is not the closest to the camera station. The RMSE for the 7 stems analysed was 1.46 cm, and the standard deviation was 1.24 cm. The stem centre estimation provides the tree location in the local reference system as well as its spatial distribution; however, its accuracy was not assessed in this paper.

Table 5 presents the estimation of the same stems using the TLS technique, which can be compared with the DBHs obtained with fisheye images in Table 3. Stem 6 was not detected from the single-scan TLS because it was partly occluded by a tree standing in front of it. The RMSE for the six stems analysed was 1.53 cm, and the standard deviation was 1.52 cm. There was no dependency between the discrepancy and the measured distance from the scanner station. If stem 6 is not considered using the fisheye technique,

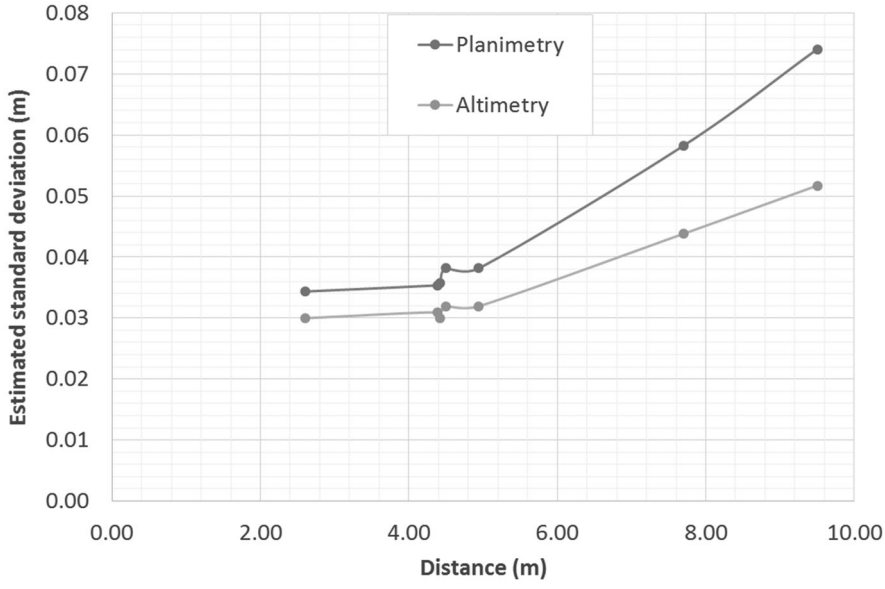

Figure 11. Planimetric and altimetric errors against the distance from the camera station to the tree stem.

Table 3. Standard deviations of the estimated parameters by circle fitting using least squares.

Stem	N. points for DBH estimation	a posteriori *sigma*	σ_X_C (m)	σ_Y_C (m)	σ_r (m)
1	5	0.002	0.008	0.003	0.006
2	7	0.015	0.016	0.047	0.008
3	18	0.015	0.014	0.011	0.013
4	5	0.010	0.025	0.012	0.025
5	11	0.002	0.004	0.001	0.004
6	9	0.002	0.031	0.013	0.024
7	9	0.004	0.008	0.002	0.007

Table 4. Validation of DBH results for seven stems.

Stem	Discrepancy (cm)	Distance between stem and camera station (m)
1	2.03	9.01
2	0.50	4.94
3	0.95	4.39
4	−2.07	7.71
5	1.56	4.42
6	1.37	4.51
7	1.02	2.60
RMSE	1.46	

Table 5. DBH estimated with the TLS technique.

Stem	Discrepancy (cm)	Distance between stem and the scanner station (cm)
1	0.31	8.49
2	−2.40	4.71
3	2.49	3.90
4	−1.41	7.67
5	−0.02	5.01
6	/	/
7	−0.02	3.11
RMSE	1.53	

then the RMSE result in Table 3 is 1.47 cm with a standard deviation of 1.32 cm.

Figure 12 shows two graphs of the discrepancies in the DBHs as a function of the distance from the acquisition station. With the fisheye technique (Figure 12(a)), the errors were less than 1.5 cm at a distance of 5 m and approximately 2 cm at distances of 5–9 m. Using the TLS technique (Figure 12(b)), the errors were less than 2.5 cm at the same distance of 5 m and approximately 1.5 cm at a distance of 7.67 m. In the comparison of both graphs, the fisheye technique resulted in discrepancies between 0.5 and 2 cm, whereas the TLS technique achieved discrepancies with a larger amplitude, varying between 0.02 and 2.50 cm, which included the largest and smallest errors. When using BA with optical images, a simultaneous network adjustment is performed for all tie points, producing an overall error minimization. For TLS, each point is defined by a single set of measurements (two angles and one single distance) without redundancy. The measurement distance did not clearly impact the accuracy of the DBH estimation; however, the distance range was quite small. Liang et al. (2015) observed that for the hand-held consumer camera used in their study, the quality of the point cloud was clearly reduced at a measurement distance of 20 m.

Some remarks can be highlighted to guarantee good results using the proposed fisheye technique:

- it is recommended to extract points covering the entire width of the stem to accurately define an arc.
- to guarantee a better approximation to a cylindrical shape, the range around the DBH used to extract points should not be too large.
- if stem shadows on the ground are also labelled in the image as a stem, the resulting 3D coordinates will be at ground level and will be discarded.

The proposed technique is applicable to trees within a camera's field of view achieved by the fisheye system position. Similar to single-scan TLS, occlusions caused by shrubs and leaves can complicate the DBH determination. However, acquiring vertical fisheye images at heights of approximately 4 m provides a viewpoint in which smaller shrubs do not hide stems at BH, which is an advantage of the vertical fisheye technique. Although the point density is not the same when using TLS, point clouds could also be generated with dense image matching and image triangulation, and objects can be partially reconstructed. This alternative could be investigated in future work. Other relevant topics for further study include the assessment of the technology in forest plots having different tree densities and tree species and the assessment of the operational range of the method.

This study presented and assessed an automatic approach based on vertical fisheye images for mapping and measuring individual tree stems. The technique considered stems as

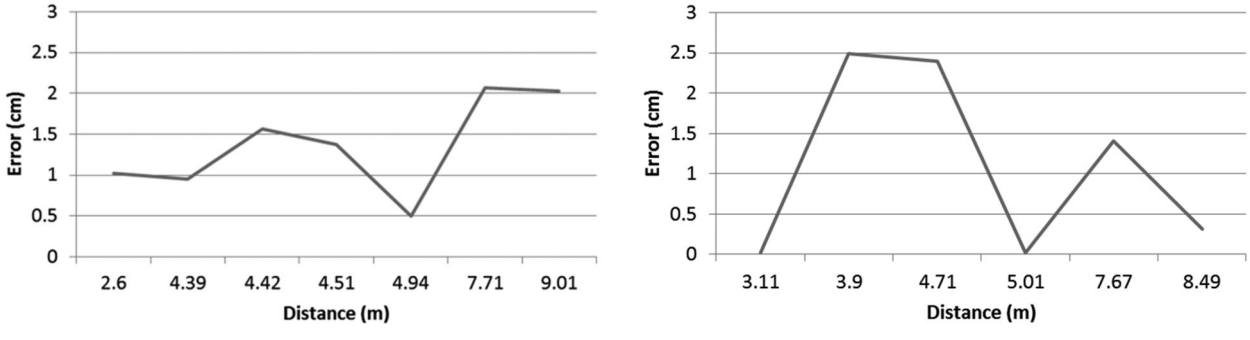

Figure 12. Graphs comparing the discrepancy against the distance from the acquisition station. Errors produced with: (a) the fisheye technique and (b) the TLS technique.

regular cylinders that were automatically located to extract point coordinates. A BA with an equidistant model enabled the estimation of the 3D coordinates of points on the stem surface. In the object space, circles were geometrically adjusted to the planimetric coordinates of each stem to determine the DBH.

Experiments were performed with a set of tree stems inside a forest sample plot. Three images were used to assess the fisheye technique in a practical field survey, which requires camera positioning and height measurements. The results showed that multi-scale images can be oriented in an arbitrary reference system without control points but using constraints imposed on the EOPs. The analysis of results indicated discrepancies with an RMSE of 1.46 cm and a standard deviation of 1.24 cm, which is compatible with the measurements manually performed on the stems. Comparable results were also verified in comparisons of discrepancies generated from a point cloud acquired by a single-scan TLS. Both are sufficiently accurate for forestry applications. With respect to the precision of the tree position mapping, the largest error obtained in the BA was 7.5 cm at a distance of approximately 10 m.

Occlusion is a major challenge for remote sensing-based techniques, for example, images and TLS. The vertical view can reduce some occlusion effects, and information about shrubs, leaves or any element on the ground can also be obtained from the panoramic images. The use of the vertical fisheye technique in dense forests can present some limitations due to occlusions. However, this problem also occurs with other optical techniques and even with TLS. Additionally, the vertical camera configuration generates point clouds from several images taken at the same location and using simple accessories, that is, a tripod with a telescopic pole. This requires less work in comparison with the point cloud generated from multi-locations, for example, paths outside a plot. Disadvantages include a shorter detection distance than TLS and the difficulty of merging several measurement positions, which is more difficult than taking images around the trees.

In this study, the main objective was to assess the technique to estimate DBHs and locate stems using a minimum number of images, which produced stem point clouds with few points, shown to be enough to provide useful values for the application. Dense stem reconstruction procedures were not addressed; they can be developed with a larger number of images to produce denser point extraction on the stem surface and to increase accuracy. In general, the approach with multi-scale fisheye images is able to capture terrestrial information that can be used for spatial location of trees and accurate determination of DBHs. Further studies can be developed for stem modelling with dense reconstruction.

Acknowledgements

The authors would like to thank the Fundação de Amparo à Pesquisa do Estado de São Paulo (FAPESP) and the Finnish Geospatial Research Institute (FGI) for assistance with the ground survey.

Disclosure statement

No potential conflict of interest was reported by the authors.

Funding

This work was supported by the Fundação de Amparo à Pesquisa do Estado de São Paulo (FAPESP) [grants number 2013/50426-4 and 2014/05033-7]

References

Berveglieri A, Oliveira RA, Tommaselli AMG. 2014. A feasibility study on the measurement of tree trunks in forests using multi-scale vertical images. In: International archives of the photogrammetry, remote sensing and spatial information sciences, ISPRS Technical Commission V Symposium, Riva del Garda, Italy; p. 87–92.

Brown DC. 1971. Close-range calibration. Photogramm Eng. 37:855–866.

Clark NA, Wynne RH, Schmoldt DL, Winn MF. 2000. An assessment of the utility of a non-metric digital camera for measuring standing trees. Comput Electron Agric. 28:151–169.

Coope ID. 1993. Circle fitting by linear and nonlinear least squares. J Optim Theory Appl. 76:381–388.

Dassot M, Constant T, Fournier M. 2011. The use of terrestrial LiDAR technology in forest science: application fields, benefits and challenges. Ann For Sci. 68:959–974.

Dick AR, Kershaw JA, MacLean DA. 2010. Spatial tree mapping using photography. North J Appl For. 27:68–74.

Evans GD, Coombe DE. 1959. Hemispherical and woodland canopy photography and the light climate. J Ecol. 47:103–113.

Forsman M, Börlin N, Holmgren J. 2012. Estimation of tree stem attributes using terrestrial photogrammetry. In: International archives of photogrammetry and remote sensing. XXII ISPRS Congress. ISPRS, Melbourne; p. 261–265.

Forsman M, Börlin N, Holmgren J. 2016. Estimation of tree stem attributes using terrestrial photogrammetry with a camera rig. Forests. 7:61–81.

Garrido-Jurado S, Muñoz-Salinas R, Madrid-Cuevas FJ, Marín-Jiménez MJ. 2014. Automatic generation and detection of highly reliable fiducial markers under occlusion. Pattern Recognit. 47:2280–2292.

Hapca AI, Mothe F, Leban J-M. 2007. A digital photographic method for 3D reconstruction of standing tree shape. Ann For Sci. 64:631–637.

Henning JG, Radtke PJ. 2006. Ground-based laser imaging for assessing three-dimensional forest canopy structure. Photogramm Eng Remote Sens. 72:1349–1358.

Herrera PJ, Pajares G, Guijarro M, Ruz JJ, Cruz JM. 2011. A stereovision matching strategy for images captured with fish-eye lenses in forest environments. Sensors. 11:1756–1783.

Kittler J, Illingworth J. 1986. Minimum error thresholding. Pattern Recognit. 19:41–47.

Korpela I, Tuomola T, Välimäki E. 2007. Mapping forest plots: an efficient method combining photogrammetry and field triangulation. Silva Fenn. 41:457–469.

Kraus K. 1993. Photogrammetry: fundamentals and standard processes. Köln: Dümmler.

Liang X, Hyyppä J. 2013. Automatic stem mapping by merging several terrestrial laser scans at the feature and decision levels. Sensors. 13:1614–1634.

Liang X, Jaakkola A, Wang Y, Hyyppä J, Honkavaara E, Liu J, Kaartinen H. 2014. The use of a hand-held camera for individual tree 3D mapping in forest sample plots. Remote Sens. 6:6587–6603.

Liang X, Litkey P, Hyyppa J, Kaartinen H, Vastaranta M, Holopainen M. 2012. Automatic stem mapping using single-scan terrestrial laser scanning. IEEE Trans Geosci Remote Sens. 50:661–670.

Liang X, Wang Y, Jaakkola A, Kukko A, Kaartinen H, Hyyppä J, Honkavaara E, Liu J. 2015. Forest data collection using terrestrial image-based point clouds from a handheld camera compared to terrestrial and personal laser scanning. IEEE Trans Geosci Remote Sens. 53:5117–5132.

Lindberg E, Holmgren J, Olofsson K, Olsson H. 2012. Estimation of stem attributes using a combination of terrestrial and airborne laser scanning. Eur J For Res. 131:1917–1931.

Lovell JL, Jupp DLB, Newnham GJ, Culvenor DS. 2011. Measuring tree stem diameters using intensity profiles from ground-based scanning lidar from a fixed viewpoint. ISPRS J Photogramm Remote Sens. 66:46–55.

Lowe DG. 2004. Distinctive image features from scale-invariant keypoints. Int J Comput Vis. 60:91–110.
Lowe DG. 2005. Demo software: SIFT keypoint detector. [cited 2015 Nov 9]. Available from: http://www.cs.ubc.ca/~lowe/keypoints/
Marcato Junior J, Moraes MVA, Tommaselli AMG. 2015. Experimental assessment of techniques for fisheye camera calibration. Bol Ciênc Geodésicas. 21:637–651.
Mikhail EM, Bethel JS, McGlone CJ. 2001. Introduction to modern photogrammetry. New York: Wiley.
Ringdahl O, Hohnloser P, Hellström T, Holmgren J, Lindroos O. 2013. Enhanced algorithms for estimating tree trunk diameter using 2D laser scanner. Remote Sens. 5:4839–4856.
Rodríguez-García C, Montes F, Ruiz F, Cañellas I, Pita P. 2014. Stem mapping and estimating standing volume from stereoscopic hemispherical images. Forstwiss Cent. 133:895–904.
Ruy R, Tommaselli AMG, Galo M, Hasegawa JK, Reis TT. 2009. Evaluation of bundle block adjustment with additional parameters using images acquired by SAAPI system. In: Proceedings of 6th international symposium on mobile mapping technology. Presidente Prudente, Brazil.
Schneider D, Schwalbe E, Maas HG. 2009. Validation of geometric models for fisheye lenses. ISPRS J Photogramm Remote Sens. 64:259–266.
Silva SLA, Tommaselli AMG, Artero AO. 2014. Utilização de alvos codificados na automação do processo de calibração de câmaras. Bol Ciênc Geodésicas. 20:636–656.
Tommaselli AMG, Berveglieri A. 2014. Automatic orientation of multi-scale terrestrial images for 3D reconstruction. Remote Sens. 6:3020–3040.
Vastaranta M, Melkas T, Holopainen M, Kaartinen H, Hyyppä J, Hyyppä H. 2009. Laser-based field measurements in tree-level forest data acquisition. Photogramm J Finl. 21:51–61.
Watt PJ, Donoghue DNM. 2005. Measuring forest structure with terrestrial laser scanning. Int J Remote Sens. 26:1437–1446.
Wolf PR, Dewitt BA, Wilkinson BE. 2014. Elements of photogrammetry with applications in GIS. 4th ed. New York: McGraw-Hill.
Yen J-C, Chang F-J, Chang S. 1995. A new criterion for automatic multilevel thresholding. IEEE Trans Image Process. 4:370–378.